HHS Public Access

Author manuscript

Investig Magn Reson Imaging. Author manuscript; available in PMC 2018 March 06.

Published in final edited form as:

Investig Magn Reson Imaging. 2017 December ; 21(4): 210–222. doi:10.13104/imri.2017.21.4.210.

Highly Accelerated SSFP Imaging with Controlled Aliasing in Parallel Imaging and integrated-SSFP (CAIPI-iSSFP)

Thomas Martin[1], **Yi Wang**[2], **Shams Rashid**[1], **Xingfeng Shao**[3], **Steen Moeller**[4], **Peng Hu**[1], **Kyunghyun Sung**[1], and **Danny JJ Wang**[3]

[1]Department of Radiological Sciences, University of California Los Angeles, California, USA

[2]Philips, MR Clinical Science NA, Florida, USA

[3]Laboratory of FMRI Technology (LOFT), Stevens Neuroimaging and Informatics Institute, University of Southern California, California, USA

[4]Center of Magnetic Resonance Research, University of Minnesota, Minnesota, USA

Abstract

Purpose—To develop a novel combination of controlled aliasing in parallel imaging results in higher acceleration (CAIPIRINHA) with integrated SSFP (CAIPI-iSSFP) for accelerated SSFP imaging without banding artifacts at 3T.

Materials and Methods—CAIPI-iSSFP was developed by adding a dephasing gradient to the balanced SSFP (bSSFP) pulse sequence with a gradient area that results in 2π dephasing across a single pixel. Extended phase graph (EPG) simulations were performed to show the signal behaviors of iSSFP, bSSFP, and RF-spoiled gradient echo (SPGR) sequences. *In vivo* experiments were performed for brain and abdominal imaging at 3T with simultaneous multi-slice (SMS) acceleration factors of 2, 3 and 4 with CAIPI-iSSFP and CAIPI-bSSFP. The image quality was evaluated by measuring the relative contrast-to-noise ratio (CNR) and by qualitatively assessing banding artifact removal in the brain.

Results—Banding artifacts were removed using CAIPI-iSSFP compared to CAIPI-bSSFP up to an SMS factor of 4 and 3 on brain and liver imaging, respectively. The relative CNRs between gray and white matter were on average 18% lower in CAIPI-iSSFP compared to that of CAIPI-bSSFP.

Conclusion—This study demonstrated that CAIPI-iSSFP provides up to a factor of four acceleration, while minimizing the banding artifacts with up to a 20% decrease in the relative CNR.

Correspondence to: Danny JJ Wang, PhD, MSCE, Department of Neurology, University of Southern California, 2025 Zonal Ave Los Angeles, CA 90032, USA, **Tel**. +310-983-3667, **Fax**. +310-794-7406, jwang71@gmail.com.

Keywords

CAIPI-iSSFP; CAIPI-bSSFP; CAIPIRINHA; Extended phase graphs (EPG); Simultaneous multi-slice (SMS)

INTRODUCTION

Balanced steady-state free precession (bSSFP) is one of the most widely used magnetic resonance imaging (MRI) pulse sequences. Due to its high signal-to-noise ratio (SNR) efficiency (1–4) and its unique tissue contrast (5, 6), bSSFP has found many applications in cardiovascular, musculoskeletal and functional MRI (4). However, similar to other steady-state imaging techniques, the imaging speed of bSSFP is still limited especially for wide volume coverage. Another limitation of bSSFP is the banding artifacts that are commonly present in imaging due to its sensitivity to off-resonance effects.

Parallel imaging is one of the most commonly used techniques for accelerated image acquisition. However, parallel imaging suffers from SNR penalties due to coil geometry (g-factor) and an undersampling of k-space lines (7, 8). Simultaneous multi-slice acquisition (SMS) has been developed as an alternative accelerated imaging method (9) by employing a superposition of radio-frequency (RF) pulses to simultaneously excite multiple slices. The advantage of using SMS over parallel imaging techniques is the minimal SNR penalty due to the full acquisition of k-space lines (10). However, if the simultaneously acquired slices are adjacent to each other, SMS can result in an incoherent reconstructed image (11). Controlled aliasing in parallel imaging that results in higher acceleration (CAIPIRINHA) (11) is a variant of the SMS technique that uses phase modulated RF pulses to excite multiple slices while simultaneously shifting the field-of-view (FOV) of the simultaneously excited slices. It can be used to improve the reconstruction of the adjacent slices and SNR.

The application of CAIPIRINHA in bSSFP imaging, however, has been limited because the phase modulation of CAIPIRINHA not only results in a spatial shift of the imaging slices, but also yields a frequency shift on the off-resonance profile of bSSFP signals and banding artifacts in simultaneously excited slices. Stäb et al. (12) proposed a technique to achieve a SMS factor of two for bSSFP imaging by shifting the center frequency of the bSSFP to yield an off-resonance angle of $\pm \pi/2$ for the two simultaneously excited imaging slices respectively, as a tradeoff between achieving SMS acceleration and minimizing banding artifacts. However, expanding such a technique to accelerated bSSFP imaging with SMS factors greater than 2 is challenging (1, 3, 4). Phase cycling may be applied to reduce the banding artifacts in CAIPI-bSSFP, however the increased scan time will discount the SNR efficiency of bSSFP and make it impractical for clinical applications. This issue is the main limitation for the application of CAIPIRINHA in bSSFP imaging, especially with high SMS acceleration factors (≥ 3).

In this study, we present a special case of the SSFP-FID sequences termed integrated SSFP (iSSFP) that removes the sensitivity of the bSSFP signals to off-resonance by using an additional gradient to dephase the spins in a pixel across a 2π cycle (13, 14). We demonstrated that there was similar tissue contrast between the two sequences by conducting

numerical simulations and performing brain and abdominal imaging, where banding often occurs. Due to the dephasing gradient, there were flow-related artifacts. The addition of flow compensated gradients made it feasible to improve the iSSFP signal in the presence of blood flow. We also combined iSSFP with CAIPIRINHA, herein termed CAIPI-iSSFP, to achieve highly accelerated SSFP imaging (acceleration factors ≥ 3). Combining these two techniques made high acceleration achievable while still removing banding artifacts and maintaining sufficient T2/T1 contrast of bSSFP.

MATERIALS AND METHODS

iSSFP with CAIPIRINHA (CAIPI-iSSFP)

The iSSFP sequence, as shown in Figure 1, is based on a previously proposed idea (i.e., an additional dephasing gradient is applied to bSSFP to fully dephase spins across a 2π cycle within a single pixel), but has not been systematically studied yet (13–16). In a nutshell, the iSSFP method integrates a 2π cycle of the bSSFP signal profile into the width of a single pixel (Fig. 1b), which eliminates its sensitivity to off-resonance. The dephasing gradient can be applied along any direction, but for the sake of simplicity, in this study, the application of the gradient along the readout or x-direction is described. The strength of the gradient is determined by the phase dispersion equation:

$$\Delta\Phi=\gamma\Delta x\int_0^{TR}G_x(t)dt \quad [1]$$

where $\Delta\Phi$ is the amount of desired phase dispersion per pixel (2π), γ is the Larmor frequency, G_x is the magnitude of the dephasing gradient, and Δx is the width of the pixel. The integral of G_x over TR is simply the 0^{th} moment or area of the dephasing gradient. Having the spins dephase across 2π within a single pixel will result in the averaging of the bSSFP signal profile (14). The advantage of this approach is that it removes the dependence of off-resonance effects, however the iSSFP signal decreases compared to the bSSFP signal. Nevertheless, iSSFP largely preserves the unique T_2/T_1 contrast of bSSFP since it averages the bSSFP signal profile.

As mentioned, iSSFP is a special case of the SSFP-FID sequences. However, it is important to differentiate iSSFP from the other types of gradient echo sequences. If the dephasing gradient area is further increased or is also applied along other directions, then the phase dispersion will increase and ultimately spoil the signal. The sequences that use these gradients that are applied in multiple directions and/or with a larger gradient area (causing a 4π or greater phase dispersion) to spoil the transversal magnetization are called gradient-spoiled echo (GRE) or RF spoiled gradient echo (SPGR) when accompanied by RF spoiling (14, 17–19). Reducing the area of the spoiling gradient such that the resultant phase dispersion is less than 2π will cause steady-state SSFP-FID and SSFP-Echo signals with complicated spin phase pathways (20). Also the signal is still dependent on off-resonance effects and may present banding artifacts. This category of pulse sequences is commonly known as a steady state gradient echo such as fast imaging with steady-state free precession (FISP) and gradient recalled acquisition in the steady state (GRASS).

Since iSSFP is not sensitive to off-resonance, accelerated SSFP imaging can be achieved by combining iSSFP and CAIPIRINHA, herein termed as CAIPI-iSSFP, with a high SNR efficiency and T_2/T_1 contrast that is similar to that of bSSFP (12, 21). The added dephasing gradient removes the inherent flow compensation of bSSFP along the direction of the applied gradient and can cause the iSSFP signal to be susceptible to blood flow artifacts. While this is not as much of an issue in the brain, the flow artifacts are more severe in body applications. Flow compensation is a technique to overcome the additional phase accrual caused by velocity (M1) and acceleration (M2) motion of the spins in the blood vessels (22–24). The M2 flow artifacts were assumed to be negligible; so, MI flow compensation was performed by adding bipolar gradients (Fig. 1) after the dephasing gradient to reduce the flow artifacts and improve the tissue signal (22, 23).

Numerical Simulations

Extended phase graph (EPG) (25) simulations of the iSSFP sequence were performed to assess its signal profile as a function of the off-resonance frequency and flip angle (FA) using custom MATLAB (The MathWorks, Natick, MA, USA) programs. For comparison, simulations were also performed for the bSSFP and SPGR sequences. The following parameters were used in the simulations: TR = 4 ms, TE = TR/2, T_1 = 1331 ms and T_2 = 80 ms for gray matter (GM), T_1 = 832 ms and T_2 = 110 ms for white matter (WM) (26), T_1 = 809 ms and T_2 = 34 ms for liver, T_1 = 1627 ms and T_2 = 34 ms for venous blood (VB), FA = 30° when simulating off-resonance and a range of 0–50° when simulating FA dependency. The numerically simulated off-resonance range was −360°/TR to 360°/TR.

In Vivo Imaging: Brain

Seven healthy volunteers (age range: 27 ± 4 years; 6 male, 1 female) provided informed consent according to a protocol approved by the local Institutional Review Board (IRB). All brain studies were performed on a Siemens TIM Trio 3T scanner (Erlangen, Germany) using a 32-channel head receiver coil. A whole brain scan was performed on each subject to demonstrate the susceptibility of banding artifacts that are common in the nasal cavity and ear canal with bSSFP sequences and the removal of the artifacts with iSSFP. Each subject was scanned using CAIPI-bSSFP and CAIPI-iSSFP with SMS factors of 1, 2, 3, and 4. Each SMS pulse excited multiple imaging slices with a relative shift spaced evenly along the phase encoding direction, i.e., a relatively spatial shift of FOV/2, FOV/3 and FOV/4 for SMS factors of 2, 3 and 4, respectively. The inter-slice gaps between the simultaneously excited slices were 72 mm, 48 mm, and 36 mm for SMS factor of 2, 3, and 4, respectively.

The common imaging parameters were: 24 slices with a thickness of 5 mm, with a gap of 1 mm between slices, matrix size = 192 × 192, FOV = 256 × 256 mm^2, repetition time (TR) = 4.2 ms and 8.4 ms, echo time (TE) = TR/2, and FA = 30°. The total scan time for the CAIPI-iSSFP and CAIPI-bSSFP scans with a SMS factor of 1, 2, 3, and 4 were 19.7, 9.8, 6.6, and 4.9 seconds, respectively. For comparison, a SPGR scan without SMS acceleration was performed with identical imaging parameters as those of the SSFP scans except TR = 366 ms, TE = 1.23 ms, FA = 7°. All CAIPI-iSSFP and CAIPI-bSSFP images were reconstructed offline using a slice-GRAPPA reconstruction algorithm implemented by using custom

MATLAB programs (27); whereas, single-band SPGR, iSSFP and bSSFP images were reconstructed online by vendor programs.

The regions-of-interest (ROIs) were manually drawn in the GM and WM, and the ventricles determined the relative contrast-to-noise ratio (CNR) of GM, WM, and cerebrospinal fluid (CSF) for SPGR, CAIPI-bSSFP, and CAIPI-iSSFP signals. The relative CNR was calculated by:

$$\mathrm{CNR}_{1\_2}=\frac{|\mathrm{S}_1-\mathrm{S}_2|}{\sigma} \quad [2]$$

where S_1 and S_2 are the signals from tissues 1 and 2, respectively, and σ is the standard deviation of the background. A ROI was drawn on the image background while avoiding ghosting or leakage artifacts to estimate the standard deviation of the noise. A two-way ANOVA statistical analysis was performed to determine if there was a significant difference of the measured relative CNR between the bSSFP and iSSFP sequences and across the four SMS factors.

In Vivo Imaging: Abdomen

A healthy volunteer (39-year-old man) underwent an abdominal MRI to evaluate the artifact removal of CAIPI-iSSFP on liver images compared to CAIPI-bSSFP as well as the MI flow compensation improvement on iSSFP. The volunteer was scanned on a Siemens Prisma 3T scanner (Erlangen, Germany) using a 30-channel body array coil. Due to the fewer channels of the body array coil, only SMS factors of 2 (FOV/2 shift) and 3 (FOV/3 shift) were achieved for CAIPI-iSSFP and CAIPI-bSSFP. The inter-slice gaps were 54 mm and 36 mm for the SMS factor of 2 and 3, respectively. In addition, an MI flow compensated iSSFP image without CAIPIRINHA was obtained to display the feasibility of signal improvement.

The common imaging parameters were: 12 slices with a thickness of 5 mm, with a gap of 4 mm between slices, matrix size = 192 × 192, FOV = 320 × 320 mm^2, TR = 7.06 ms, TE = 3.53 ms and 1.36 ms for iSSFP without and with M1flow compensation, respectively, and FA = 60°. The total scan time for the CAIPI-iSSFP and CAIPI-bSSFP scans with SMS factors of 1, 2, and 3 were 18, 10, and 6 seconds, respectively. All scans were performed with breath hold.

RESULTS

iSSFP Imaging

Figure 2 provides the brain scans from bSSFP, iSSFP, and SPGR sequences without CAIPIRINHA acceleration. The iSSFP contrast was more similar to that of bSSFP compared to SPGR. The ventricles (CSF) and the gray and white matter contrast were comparable between the two sequences (see Slice 3). In slice 2, for the bSSFP and iSSFP images, there were bright blood signals in the internal carotid arteries (white arrows); although it was not as prominent in the SPGR sequence. In slice 2, there was also a banding

artifact in the bSSFP image that was not apparent in the SPGR and iSSFP images identified by the blue arrows.

Numerical Simulations

Figure 3 displays the simulated signals of iSSFP, bSSFP, and SPGR for the GM and WM, liver, and VB using the steady-state portion of the EPG. The simulated signal for iSSFP and SPGR did not have an off-resonance dependency, while the bSSFP signal profile varied with the off-resonance of the spins.

The FA dependency of iSSFP, bSSFP, and SPGR for the different tissue types shown in Figure 3 (top) demonstrated that the iSSFP signal was located in between the SPGR and bSSFP curves for both gray and white matter as well as liver tissue and venous blood. At a FA of 30°, which is the FA for *in vivo* imaging, there was an approximately 20% decrease in the iSSFP signal compared to the bSSFP signal. In contrast, the SPGR signal decrease was approximately 85% of the bSSFP signal at a FA of 30°.

In Vivo Imaging: Brain

Figures 4 and 5 display the brain images of simultaneously acquired slices using an SMS factor of 2, 3, and 4 using a short and long TR, respectively. In the CAIPI-bSSFP images, there were clearly visible banding artifacts near the ear canals and the nasal cavity. The banding artifacts were even more severe in the longer TR images (Fig. 5). However, CAIPI-iSSFP completely removed the banding artifacts while maintaining a good GM, WM, and CSF contrast.

Figure 6 provides the average relative CNR of all the subjects between the ventricles (CSF) and white matter (CNR_{V_WM}) and between white and gray matter (CNR_{WM_GM}) for the CAIPI-iSSFP, CAIPI-bSSFP, and SPGR sequences. The measured relative CNR was similar to the simulations such that the iSSFP signal was located between bSSFP and SPGR. The relative CNR_{WM_GM} for iSSFP was on average about 18% less than that of bSSFP, and the reduction of CNR using iSSFP was significant ($p = 0.001$). The relative CNR_{V_WM} for iSSFP was on average about 20% less than that of bSSFP ($p = 0.04$). As the SMS factor increased, the relative CNR decreased due to the increased g-factor, and the effect of SMS factor was significant for the relative CNR_{WM_GM} ($P = 0.04$) but not for the relative CNR_{V_WM} ($P = 0.57$).

In Vivo Imaging: Abdomen

Figure 7 provides the liver images acquired with CAIPI-bSSFP and CAIPI-iSSFP respectively, with an SMS factor of 3. Due to a large FOV, there were severe banding artifacts, identified by blue arrows, in the CAIPI-bSSFP images, which were completely absent in the CAIPI-iSSFP images. However, the blood signals of the portal vein and hepatic artery were largely spoiled in CAIPI-iSSFP and flow artifacts were seen in the aorta and portal vein. The figure also demonstrates that an acceleration factor up to three was achievable for abdominal imaging. The flow compensation appeared to restore some of the lost signal compared to CAIPI-iSSFP (red arrows), as well as reduce the flow artifacts in the aorta and portal vein.

Figure 8 provides the images at the same window and leveling that was acquired by using bSSFP, iSSFP with and without flow compensation, and SPGR respectively. The bSSFP image had the brightest signal of VB and overall tissue contrast, but there was a signal dropout near the edges of the different organs, particularly around the stomach area. The banding artifacts were removed in the iSSFP images; however, the flow artifacts were present in the portal vein and aorta regions. Furthermore, iSSFP had a more similar contrast to bSSFP than to SPGR especially when the flow compensation was applied.

DISCUSSION

This study presented an SMS SSFP imaging technique by combining an iSSFP sequence with CAIPIRINHA to achieve an acceleration factor up to four for brain imaging and three for abdominal imaging while removing banding artifacts. By adding a 2Π dephasing gradient after the readout gradient, the phases of the spins within a single pixel were evenly spread across 2Π, thereby averaging the bSSFP signal profile and effectively removing the off-resonance dependency. Another advantage of iSSFP is that it maintains the similar T_2/T_1 contrast of bSSFP as exhibited by both simulations and in *vivo* experiments. This unique T_2/T_1 contrast was particularly useful for imaging tissues with a high T_2/T_1 ratio such as CSF and blood.

Compared to phase cycled bSSFP imaging with multiple acquisitions, iSSFP did not increase the scan time nor require advanced post-processing algorithms, such as the elliptical model (28). Since MRI is trending towards a higher magnetic field strength, the banding artifacts may become a major challenge for bSSFP imaging particularly when a wide volumetric coverage is required. The iSSFP sequence offers a simple solution to remove the banding artifacts by turning on a dephasing gradient in a standard bSSFP sequence. Due to its technical simplicity and robustness, iSSFP can be implemented easily as an option for bSSFP sequences. The utility of iSSFP was recently demonstrated in 7T functional MRI and interventional MRI applications (29, 30). It is also possible for iSSFP to be implemented in other CAIPIRINHA techniques to improve the SNR instead of using a T1-weighted image (31–34).

It is worth noting that iSSFP is a special case of the SSFP-FID sequences and was based on a previously proposed idea (13–16). However, it is different from the gradient echo sequences such as FISP or GRASS which employs no or only a small spoiling gradient (phase dispersion < 2Π). The spin pathways in steady state gradient echo sequences are highly complicated including contributions from longitudinal and transversal magnetization and stimulated echo. These sequences are also sensitive to field inhomogeneity effects. We tested FISP scans (images not shown) by eliminating the rephasing gradient in the bSSFP sequence, and the results displayed striping artifacts probably due to the sensitivity of FISP to the background gradient. In contrast, all iSSFP scans performed in our experiment exhibited excellent image quality without banding or striping artifacts.

We demonstrated that the banding artifacts could also be removed from abdominal imaging by using CAIPI-iSSFP, which is a major limitation of the application of bSSFP in the body. CAIPIRINHA can be used to accelerate the image acquisition without compromising the

SNR compared to other parallel imaging techniques. However, with the added dephasing gradient, the net gradient area was non-zero, and the inherent flow compensation of bSSFP no longer existed along the direction that the dephasing gradient was applied. This outcome may have caused signal voids for flowing spins in that direction (35) as seen in Figures 7 and 8. Composite bipolar gradients were applied in iSSFP for the liver images to satisfy both requirements in terms of the 0^{th} (2Π phase dispersion) and 1^{st} moments (0 for flow compensation). The flow artifacts were decreased, and some signal was restored, but the tissue contrast was still less than the bSSFP sequence, which was expected.

By exploiting the inherent phase modulation of CAIPIRINHA, a phase-cycled CAIPI-bSSFP technique was recently introduced that acquires multiple phase-cycled bSSFP images without a prolonged scan time compared to a standard bSSFP scan (36). This phase-cycled CAIPI-bSSFP technique, while successful for reducing/minimizing banding artifacts, has limited capability to achieve an accelerated image acquisition. The proposed CAIPI-iSSFP technique can simultaneously achieve accelerated image acquisition and removal of banding artifacts.

Other challenges of CAIPI-iSSFP include an increased specific absorption ratio (SAR) of RF power especially when the FA is greater than 40°. A simple solution would be to lengthen the RF duration and TR. The current experiment increased the TR to 8.4 ms with a larger FA. The results displayed a dramatic increase of the banding artifacts in CAIPI-bSSFP, which were not present in the CAIPI-iSSFP images. This result supports the robustness of the CAIPI-iSSFP technique in the presence of severe off-resonance effects. There are other alternative methods that have been proposed to reduce the RF power for SMS imaging (37), which can be applied to CAIPI-iSSFP so that the acquisition time does not need to be increased.

We performed a semi-quantitative analysis to compare the relative CNR between the CAIPI-iSSFP, CAIPI-bSSFP, and SPGR scans. As the SMS factor increased, the relative CNR decreased which was expected due to the increased g-factor, with the exception of the relative CNR between the ventricles (CSF) and white matter of the CAIPI-bSSFP sequence. The CSF signal in the ventricles varied quite dramatically (bright vs. dark), which made it difficult to manually draw the ROIs. Another limitation in measuring the CNR was that only the relative CNR was measured because the background noise for an image acquired by a 32-head receiver coil is spatially inhomogeneous.

In conclusion, we have demonstrated that CAIPI-iSSFP is a promising imaging technique that offers high acceleration without banding artifacts while maintaining sufficient tissue contrast. We were able to achieve whole brain imaging in less than 5 seconds using a simultaneous multi-slice acceleration factor up to four while removing banding artifacts and compromising on average only 18% relative CNR compared to CAIPI-bSSFP. The feasibility of CAIPI-iSSFP in the liver was demonstrated with minimal flow and banding artifacts up to a simultaneous multi-slice acceleration factor of three. Using CAIPI-iSSFP with flow compensation can lead to more widespread applications of SSFP imaging in the body.

Acknowledgments

This study was supported by NIH R01-NS081077, UH2-NS100G14, and Siemens Research Support.

References

1. Miller KL, Tijssen RH, Stikov N, Okell TW. Steady-state MRI: methods for neuroimaging. Imaging Med. 2011; 3:93–105.
2. Carr H. Steady-state free precession in nuclear magnetic resonance. Phys Rev. 1958; 112:1693–1701.
3. Bieri O, Scheffler K. Fundamentals of balanced steady state free precession MRI. J Magn Reson Imaging. 2013; 38:2–11. [PubMed: 23633246]
4. Scheffler K, Lehnhardt S. Principles and applications of balanced SSFP techniques. Eur Radiol. 2003; 13:2409–2418. [PubMed: 12928954]
5. Oppelt A, Graumann R, Barfuß H, Fischer H, Hartl W, Schajor W. FISP: a new fast MRI sequence. Electromedica. 1986; 54:15–18.
6. Duerk JL, Lewin JS, Wendt M, Petersilge C. Remember true FISP? A high SNR, near 1-second imaging method for T2-like contrast in interventional MRI at .2 T. J Magn Reson Imaging. 1998; 8:203–208. [PubMed: 9500281]
7. Pruessmann KP, Weiger M, Scheidegger MB, Boesiger P. SENSE: sensitivity encoding for fast MRI. Magn Reson Med. 1999; 42:952–962. [PubMed: 10542355]
8. Robson PM, Grant AK, Madhuranthakam AJ, Lattanzi R, Sodickson DK, McKenzie CA. Comprehensive quantification of signal-to-noise ratio and g-factor for image-based and k-space-based parallel imaging reconstructions. Magn Reson Med. 2008; 60:895–907. [PubMed: 18816810]
9. Larkman DJ, Hajnal JV, Herlihy AH, Coutts GA, Young IR, Ehnholm G. Use of multicoil arrays for separation of signal from multiple slices simultaneously excited. J Magn Reson Imaging. 2001; 13:313–317. [PubMed: 11169840]
10. Setsompop K, Cohen-Adad J, Gagoski BA, et al. Improving diffusion MRI using simultaneous multi-slice echo planar imaging. Neuroimage. 2012; 63:569–580. [PubMed: 22732564]
11. Breuer FA, Blaimer M, Heidemann RM, Mueller MF, Griswold MA, Jakob PM. Controlled aliasing in parallel imaging results in higher acceleration (CAIPIRINHA) for multi-slice imaging. Magn Reson Med. 2005; 53:684–691. [PubMed: 15723404]
12. Stäb D, Ritter CO, Breuer FA, Weng AM, Hahn D, Köstler H. CAIPIRINHA accelerated SSFP imaging. Magn Reson Med. 2011; 65:157–164. [PubMed: 20872868]
13. Haacke EM, Wielopolski PA, Tkach JA, Modic MT. Steady-state free precession imaging in the presence of motion: application for improved visualization of the cerebrospinal fluid. Radiology. 1990; 175:545–552. [PubMed: 2326480]
14. Hargreaves BA. Rapid gradient-echo imaging. J Magn Reson Imaging. 2012; 36:1300–1313. [PubMed: 23097185]
15. Khajehim, M., Nasiraei-Moghaddam, A., Hossein-Zadeh, GA., Martin, T., Wang, D. A quantitative analysis of fMRI induced phase changes using averaged-BOSS (A-BOSS). In Proceedings of the 23rd Scientific Meeting of International Society for Magnetic Resonance in Medicine; Toronto. 2015. p. 3921
16. Shams, Z., Moghaddam, AN. Averaged-BOSS: feasibility study and preliminary results. In Proceedings of the 22nd Scientific Meeting of International Society for Magnetic Resonance in Medicine; Milan. 2014. p. 4216
17. Zur Y, Wood ML, Neuringer LJ. Spoiling of transverse magnetization in steady-state sequences. Magn Reson Med. 1991; 21:251–263. [PubMed: 1745124]
18. Crawley AP, Wood ML, Henkelman RM. Elimination of transverse coherences in FLASH MRI. Magn Reson Med. 1988; 8:248–260. [PubMed: 3205155]
19. Sekihara K. Steady-state magnetizations in rapid NMR imaging using small flip angles and short repetition intervals. IEEE Trans Med Imaging. 1987; 6:157–164. [PubMed: 18230442]

20. Scheffler IE, Elson EL, Baldwin RL. Helix formation by dAT oligomers. I. Hairpin and straight-chain helices. J Mol Biol. 1968; 36:291–304. [PubMed: 5760542]
21. Breuer FA, Blaimer M, Mueller MF, et al. Controlled aliasing in volumetric parallel imaging (2D CAIPIRINHA). Magn Reson Med. 2006; 55:549–556. [PubMed: 16408271]
22. Haacke EM, Lenz GW. Improving MR image quality in the presence of motion by using rephasing gradients. AJR Am J Roentgenol. 1987; 148:1251–1258. [PubMed: 3495155]
23. Axel L, Morton D. MR flow imaging by velocity-compensated/uncompensated difference images. J Comput Assist Tomogr. 1987; 11:31–34. [PubMed: 3805425]
24. Simonetti OP, Wendt RE 3rd, Duerk JL. Significance of the point of expansion in interpretation of gradient moments and motion sensitivity. J Magn Reson Imaging. 1991; 1:569–577. [PubMed: 1790382]
25. Weigel M. Extended phase graphs: dephasing, RF pulses, and echoes - pure and simple. J Magn Reson Imaging. 2015; 41:266–295. [PubMed: 24737382]
26. Wansapura JP, Holland SK, Dunn RS, Ball WS Jr. NMR relaxation times in the human brain at 3.0 tesla. J Magn Reson Imaging. 1999; 9:531–538. [PubMed: 10232510]
27. Wang Y, Moeller S, Li X, et al. Simultaneous multi-slice Turbo-FLASH imaging with CAIPIRINHA for whole brain distortion-free pseudo-continuous arterial spin labeling at 3 and 7 T. Neuroimage. 2015; 113:279–288. [PubMed: 25837601]
28. Xiang QS, Hoff MN. Banding artifact removal for bSSFP imaging with an elliptical signal model. Magn Reson Med. 2014; 71:927–933. [PubMed: 24436006]
29. Mikaiel, S., Martin, T., Sung, K., Wu, H. Real-time golden angle radial iSSFP for interventional MRI. In Proceedings of the 24th Scientific Meeting of International Society for Magnetic Resonance in Medicine; Singapore. 2016. p. 3579
30. Sun K, Xue R, Zhang P, et al. Integrated SSFP for functional brain mapping at 7T with reduced susceptibility artifact. J Magn Reson. 2017; 276:22–30. [PubMed: 28092785]
31. Kim MO, Hong T, Kim DH. Multislice CAIPIRINHA using view angle tilting technique (CAIPIVAT). Tomography. 2016; 2:43–48.
32. Kim D, Seo H, Oh C, Han Y, Park H. Multi-slice imAGe generation using intra-slice parallel imaging and Inter-slice shifting (MAGGULLI). Phys Med Biol. 2016; 61:1692–1704. [PubMed: 26836647]
33. Bilgic B, Gagoski BA, Cauley SF, et al. Wave-CAIPI for highly accelerated 3D imaging. Magn Reson Med. 2015; 73:2152–2162. [PubMed: 24986223]
34. Setsompop K, Gagoski BA, Polimeni JR, Witzel T, Wedeen VJ, Wald LL. Blipped-controlled aliasing in parallel imaging for simultaneous multislice echo planar imaging with reduced g-factor penalty. Magn Reson Med. 2012; 67:1210–1224. [PubMed: 21858868]
35. Bieri O, Scheffler K. Flow compensation in balanced SSFP sequences. Magn Reson Med. 2005; 54:901–907. [PubMed: 16142709]
36. Wang Y, Shao X, Martin T, Moeller S, Yacoub E, Wang DJ. Phase-cycled simultaneous multislice balanced SSFP imaging with CAIPIRINHA for efficient banding reduction. Magn Reson Med. 2016; 76:1764–1774. [PubMed: 26667600]
37. Gagoski BA, Bilgic B, Eichner C, et al. RARE/turbo spin echo imaging with simultaneous multislice wave-CAIPI. Magn Reson Med. 2015; 73:929–938. [PubMed: 25640187]

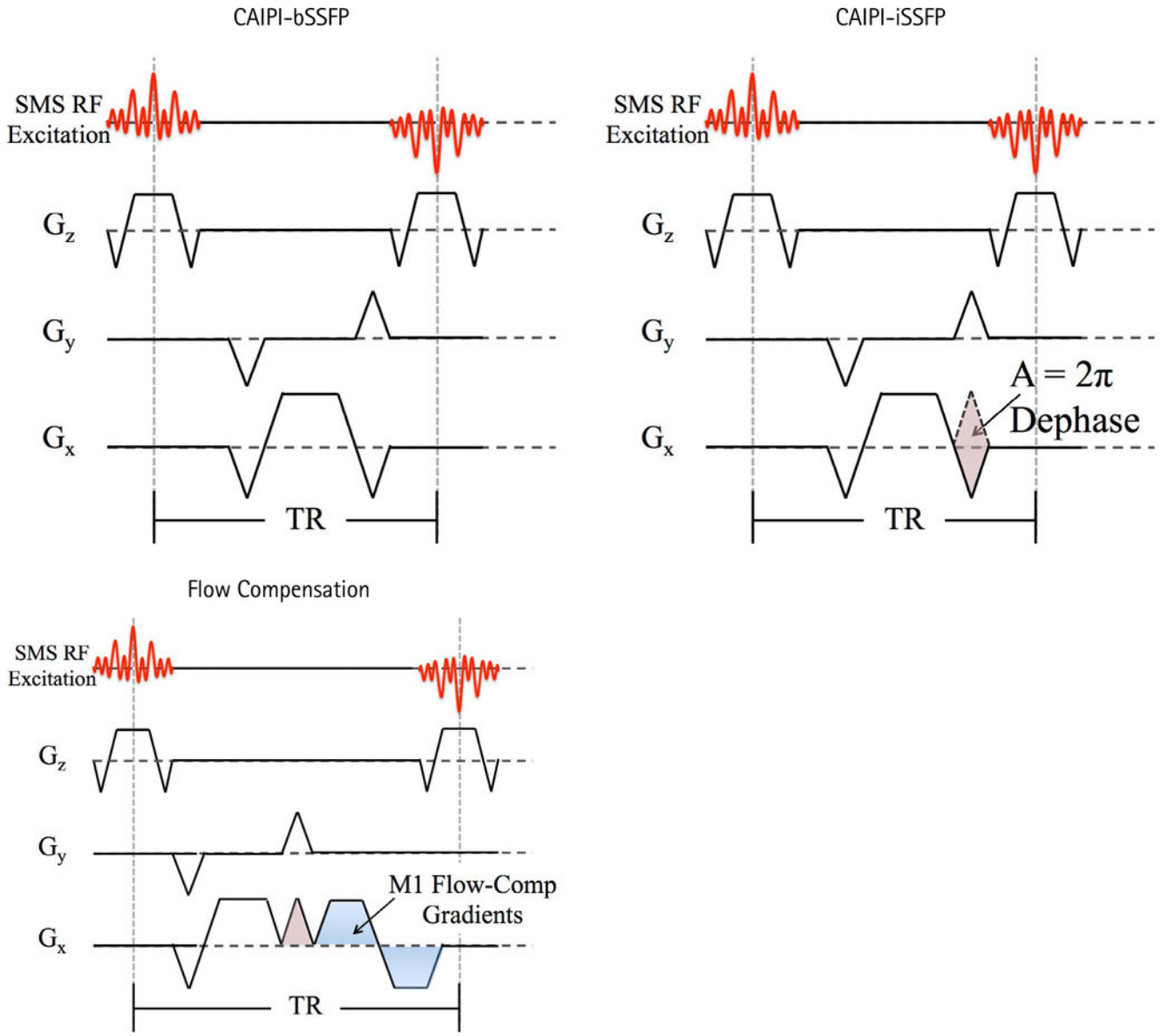

Fig. 1.

Pulse sequence diagrams for CAIPI-bSSFP (left) and CAIPI-iSSFP (right) and CAIPI-iSSFP with flow compensation gradients. CAIPI-bSSFP and CAIPI-iSSFP were the same except for the added dephasing gradient in the readout direction, where it caused a 2Π dephasing of the spins within a voxel, which resulted in an averaging of the bSSFP signal profile. To compensate for and reduce flow related artifacts and signal loss in CAIPI-iSSFP, bipolar gradients were added. CAIPI-bSSFP = controlled aliasing in parallel imaging and balanced steady-state free precession; CAIPI-iSSFP = controlled aliasing in parallel imaging and integrated SSFP; RF = radiofrequency; SMS = simultaneous multi-slice; TR = repetition time

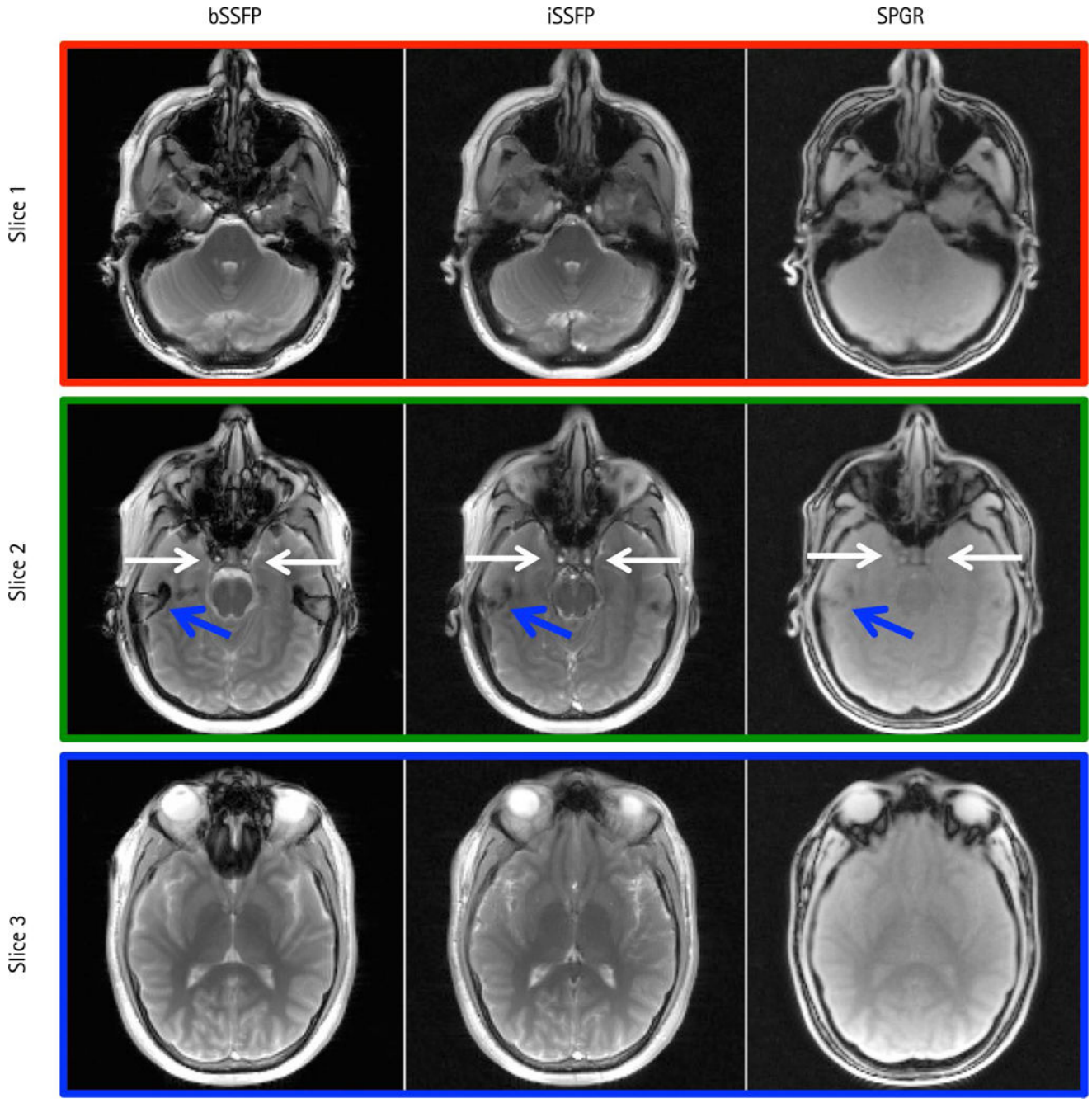

Fig. 2.

Comparison of bSSFP, iSSFP, and SPGR images without CAIPIRINHA acceleration methods. The iSSFP contrast was more similar to that of bSSFP than SPGR. White arrows indicate a blood signal that was visible in bSSFP and iSSFP, but not SPGR. Blue arrows highlight the banding artifacts in bSSFP image that were not present in iSSFP and SPGR. bSSFP = balanced steady-state free precession; CAIPIRINHA = controlled aliasing in parallel imaging results in higher acceleration; iSSFP = integrated SSFP; SPGR = spoiled gradient echo

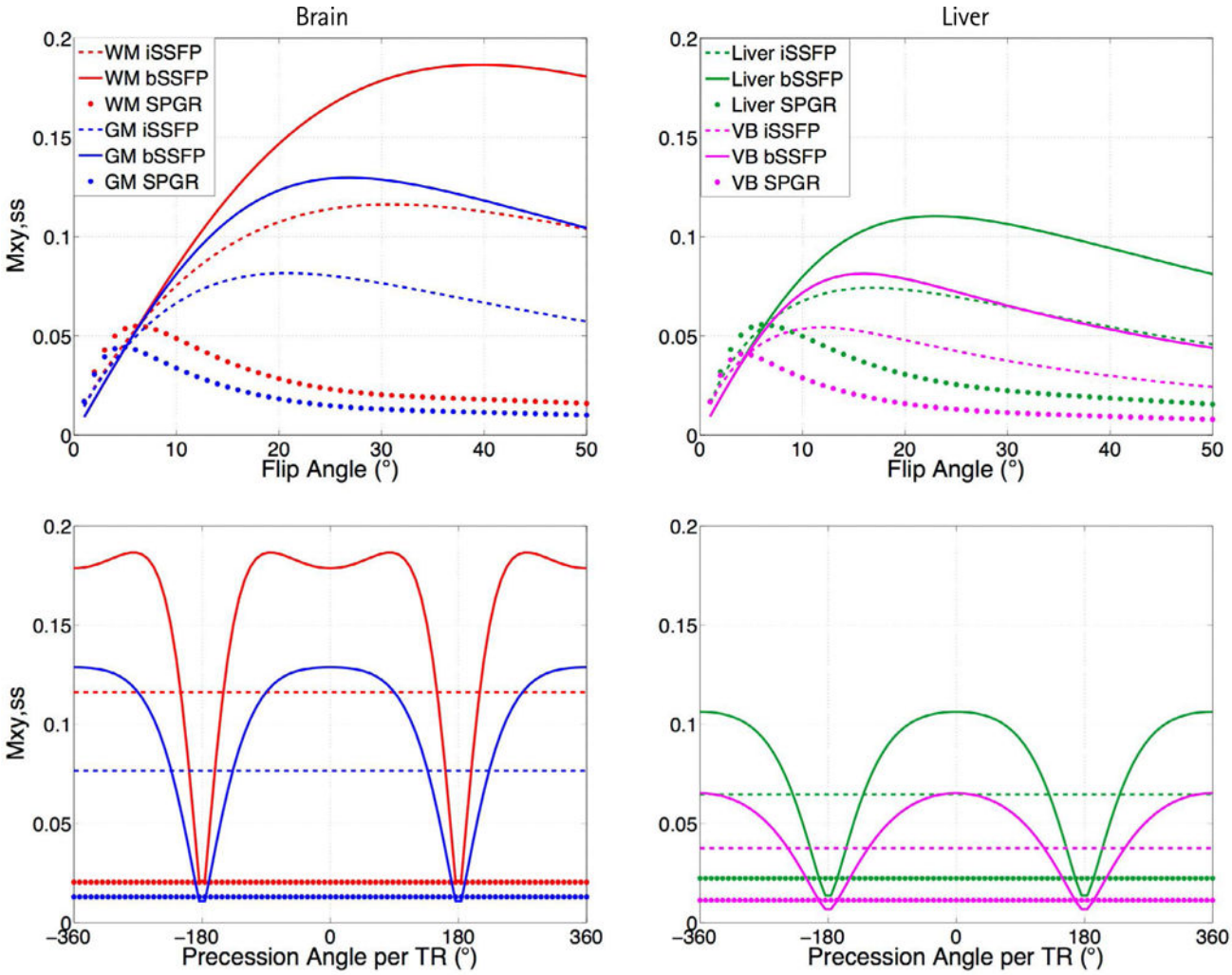

Fig. 3.

Numerical simulations plotting the signal profiles of bSSFP, iSSFP, and SPGR as a function of the flip angle (top) and off resonance (bottom) for white matter (WM), gray matter (GM), liver, and venous blood (VB). The simulated signal for iSSFP was less than bSSFP and higher than SPGR for all tissue and blood, and was not sensitive to off-resonance. bSSFP = balanced steady-state free precession; iSSFP = integrated SSFP; SPGR = spoiled gradient echo; TR = repetition time

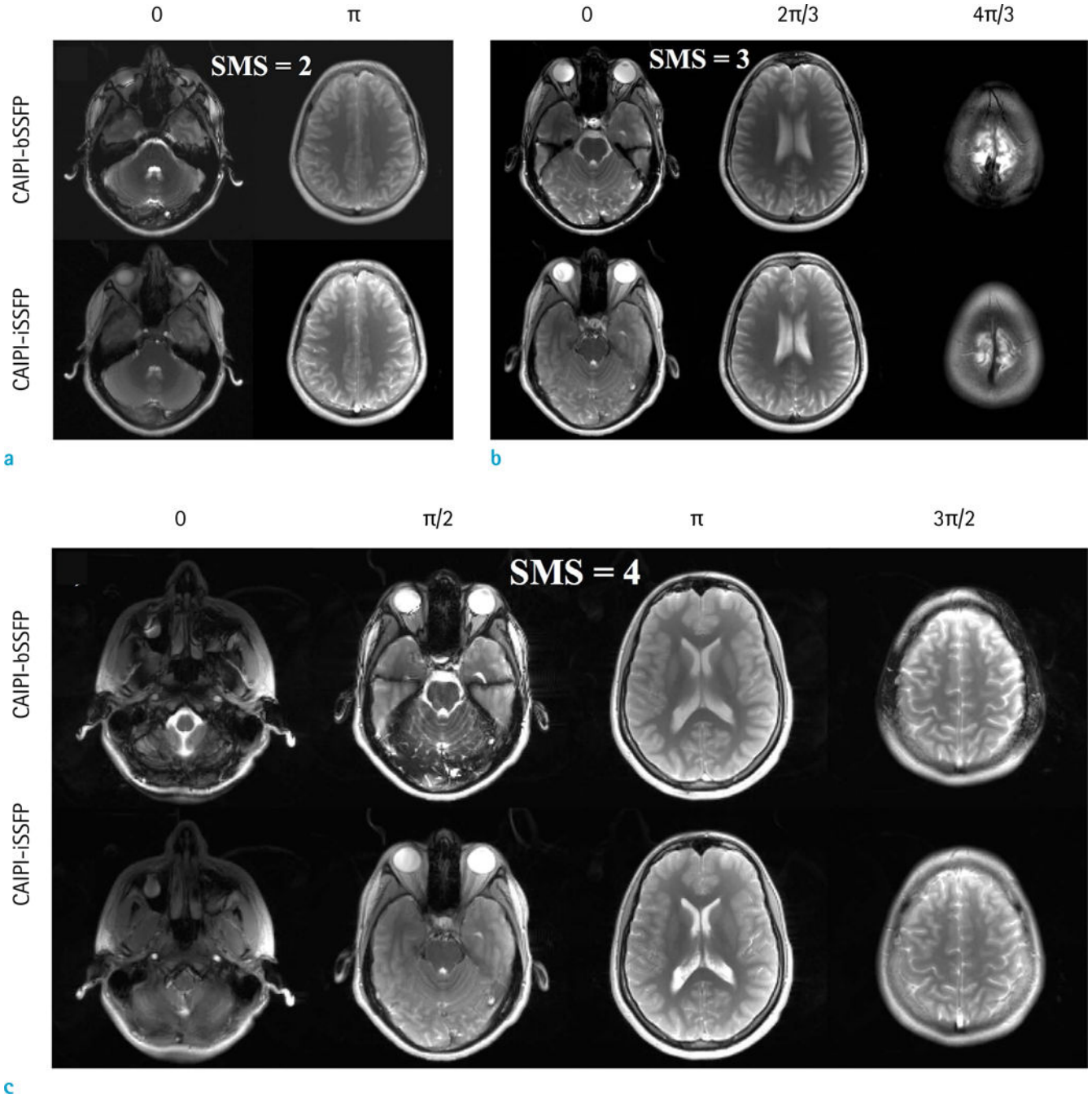

Fig. 4.

Comparison of CAIPI-iSSFP and CAIPI-bSSFP with SMS acceleration factors of 2 (a), 3 (b), and 4 (c). Examples of unaliased images from a single simultaneously excited slice are shown. The phase modulation for each of the images is shown above. There were banding artifacts clearly present in b) and c) in the phase modulations of 0 and Π/2 respectively, while in the CAIPI-iSSFP images the banding artifacts were not visible. The image contrast between the different tissues was comparable between the two sequences, and the noise did not significantly degrade the image quality with an SMS factor of 4. CAIPI-bSSFP =

controlled aliasing in parallel imaging and balanced steady-state free precession; CAIPI-iSSFP = controlled aliasing in parallel imaging and integrated SSFP; SMS = simultaneous multi-slice

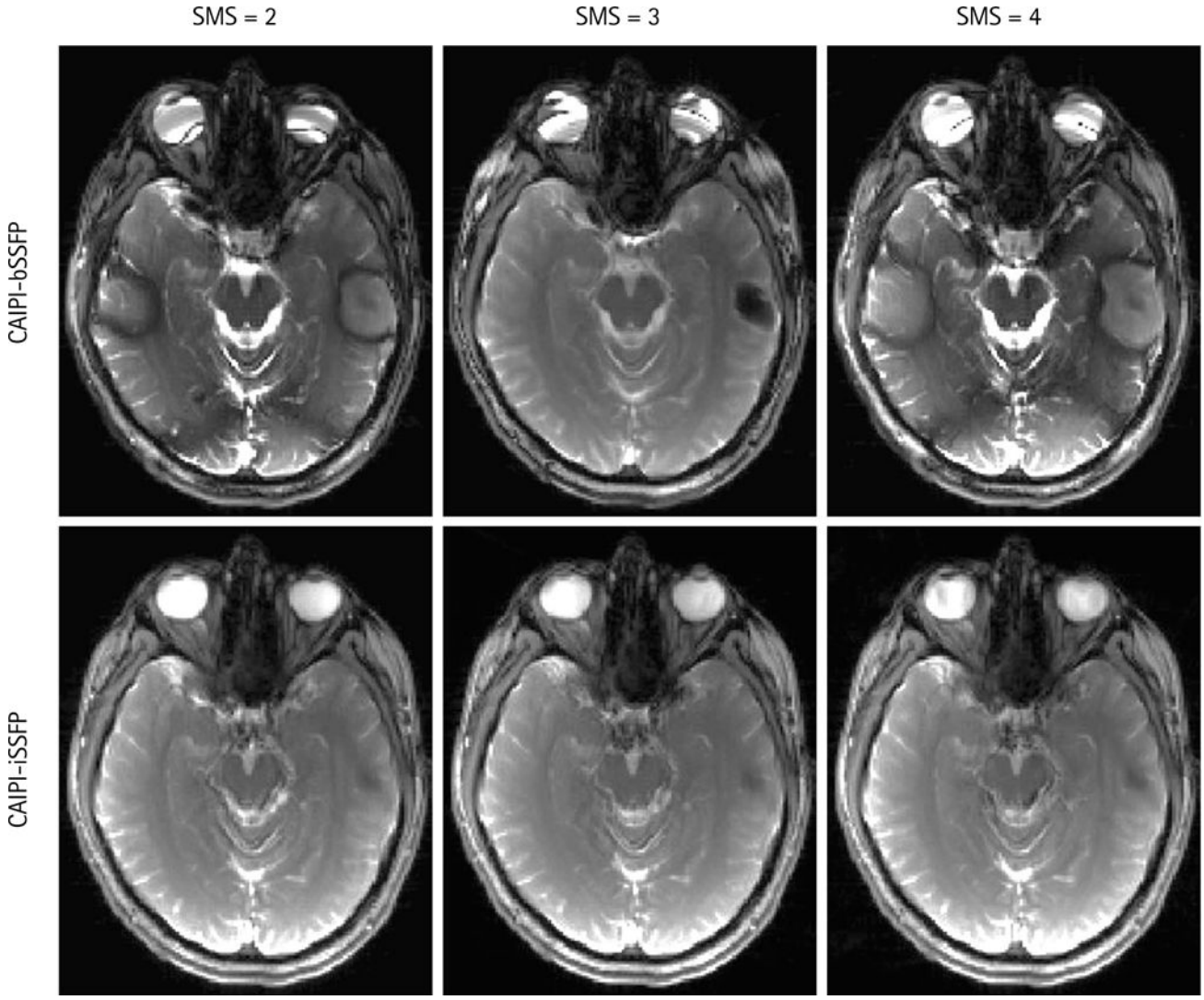

Fig. 5.

Example images showing SMS factors of 2, 3, and 4 with CAIPI-iSSFP (bottom) and CAIPI-bSSFP (top) sequences using a long TR of 8.4 ms. There were severe banding artifacts in the CAIPI-bSSFP images; whereas, the CAIPI-iSSFP images did not have banding artifacts. CAIPI-bSSFP = controlled aliasing in parallel imaging and balanced steady-state free precession; CAIPI-iSSFP = controlled aliasing in parallel imaging and integrated SSFP; SMS = simultaneous multi-slice

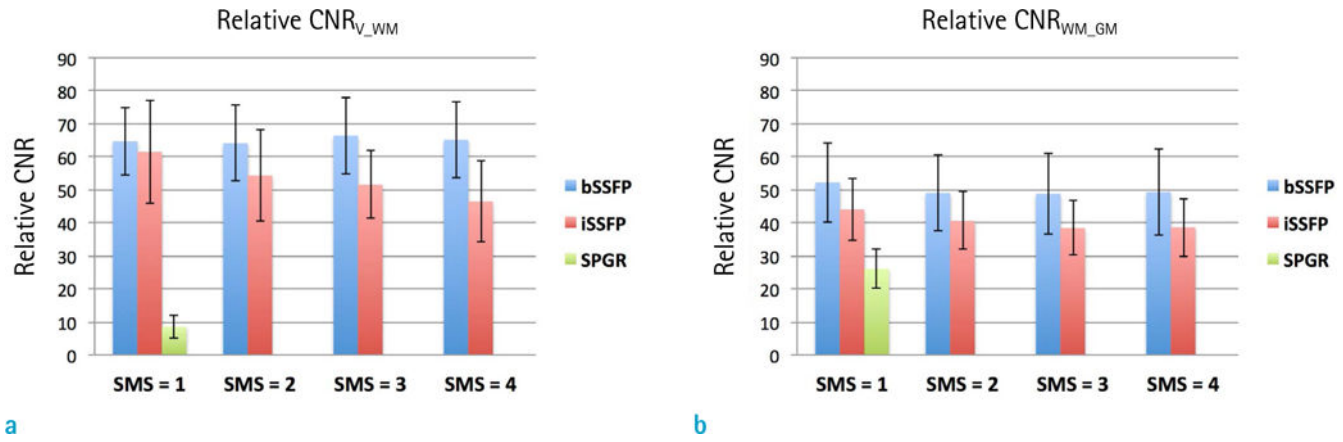

Fig. 6.

Plots showing the measured relative CNR of white matter and ventricles (a), and white and gray matter (b) for bSSFP, iSSFP, and SPGR with CAIPIRINHA acceleration SMS = 2, 3, and 4. The relative CNR was less for iSSFP compared to bSSFP, but had a much higher relative CNR than SPGR. As the SMS increased, the relative CNR decreased due to the g-factor. bSSFP = balanced steady-state free precession; CAIPIRINHA = controlled aliasing in parallel imaging results in higher acceleration; CNR = contrast-to-noise ratio; iSSFP = integrated SSFP; SMS = simultaneous multi-slice; SPGR = spoiled gradient echo

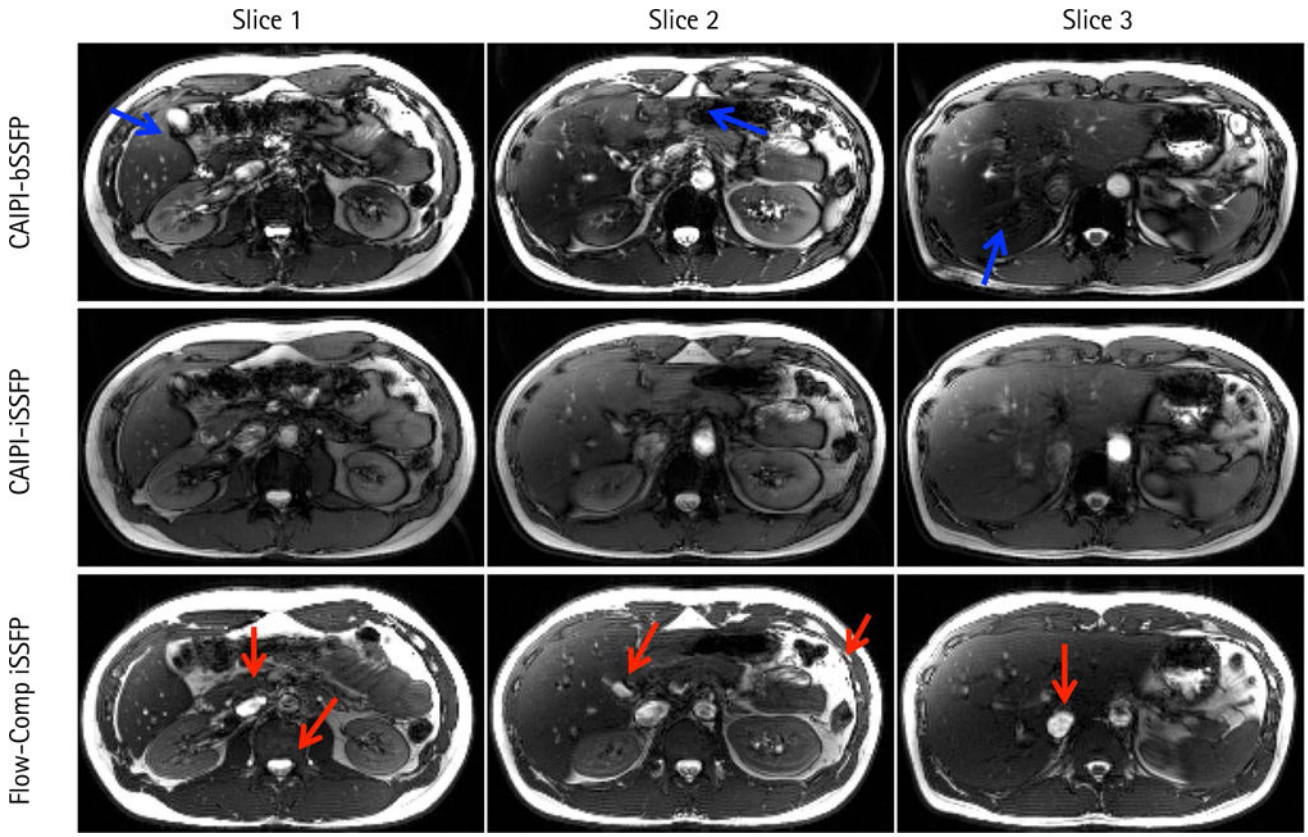

Fig. 7.

CAIPI-bSSFP and CAIPI-iSSFP with SMS factor of 3 and iSSFP with flow compensation liver scan. The blue arrows identify the banding that was present in the CAIPI-bSSFP images. Spinal fluid and VB signal was suppressed in CAIPI-iSSFP due to the spoiling. However, the banding artifacts were removed and the aorta still showed a bright signal. Adding the M1 flow compensation improved the spinal fluid and VB signal (red arrows). CAIPI-bSSFP = controlled aliasing in parallel imaging and balanced steady-state free precession; CAIPI-iSSFP = controlled aliasing in parallel imaging and integrated SSFP; SMS = simultaneous multi-slice; VB = venous blood

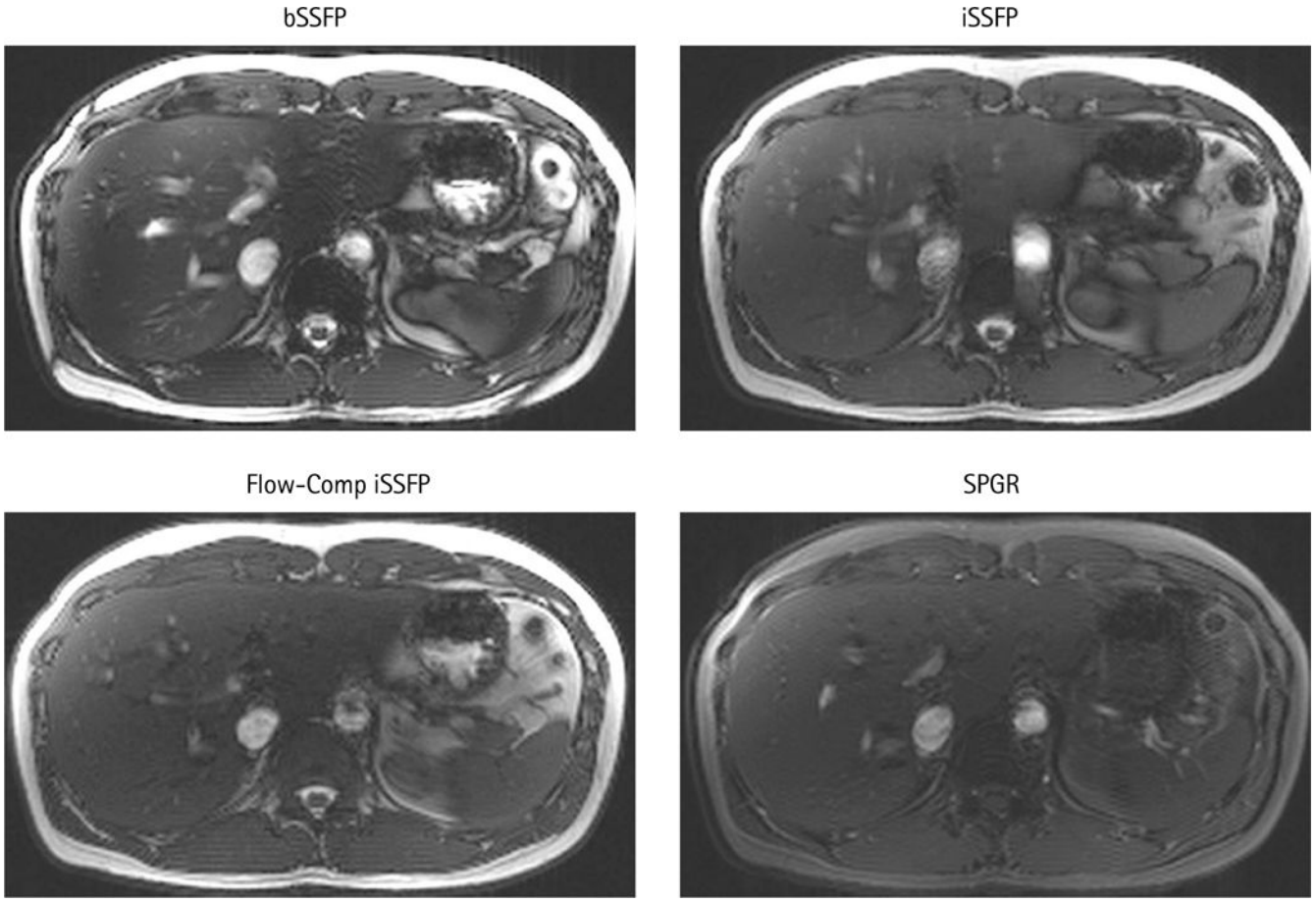

Fig. 8.

Comparison of bSSFP, iSSFP, iSSFP with M1 flow compensation, and SPGR sequence images without CAIPIRINHA in the liver. The VB signal in the iSSFP and SPGR images was significantly less due to the spoiling. However, the banding artifacts were removed compared to bSSFP. The flow compensation did improve the VB ghosting artifacts; however, some of the VB signal within the liver was not as bright. bSSFP = balanced steady-state free precession; CAIPIRINHA = controlled aliasing in parallel imaging results in higher acceleration; iSSFP = integrated SSFP; VB = venous blood